Higher-spin structures in ^{21}F and ^{25}Na

J. M. VonMoss, S. L. Tabor, Vandana Tripathi, A. Volya, B. Abromeit, P. C. Bender, D. D. Caussyn, R. Dungan, K. Kravvaris, M. P. Kuchera, R. Lubna, S. Miller, J. J. Parker, IV, and P.-L. Tai

Phys. Rev. C **92**, 034301 — Published 3 September 2015

DOI: 10.1103/PhysRevC.92.034301

Higher spin structures in ^{21}F and ^{25}Na

J. M. VonMoss[a], S. L. Tabor, Vandana Tripathi, A. Volya, B. Abromeit, P.C. Bender[b], D.D. Caussyn, R. Dungan, K. Kravvaris, M.P. Kuchera[b], R. Lubna, S. Miller, J.J. Parker IV, and P.-L. Tai

Department of Physics, Florida State University, Tallahassee, Florida 32306, USA

Abstract

Excited states were investigated in ^{21}F and ^{25}Na using the ^{9}Be(^{14}C,pnγ) reaction at 30, 35, and 45 MeV and the ^{9}Be(^{18}O,pnγ) reaction at 35 MeV. Protons were detected and identified in an E-ΔE telescope at 0^o in coincidence with one or more γ radiations in the FSU Compton-suppressed Ge detector array. Many new levels and electromagnetic decays were observed, especially among the higher spin states. Angular distributions and mean lifetimes were measured wherever possible in both nuclei. The energy levels of the positive-parity states in the two nuclei agree rather well with shell model calculations using both the USDA and WBP interactions up to the highest spins observed of 13/2 $\hbar$. Both a weak coupling approximation and shell model calculations using the WBP interaction generally reproduce the negative-parity states in ^{21}F. The shell model calculations reproduce relatively well the measured M1 and E2 transitions in both nuclei, but overpredict the parity-changing E1 transitions in ^{21}F, the only nucleus in which negative-parity states were observed in the present experiment.

I. INTRODUCTION

Both ^{21}F and ^{25}Na have odd Z (9 and 11) and two more neutrons than the stable isotopes of these elements. Most investigations of them were conducted in earlier times, with emphasis moving to the heavier, more exotic, isotopes in recent times. However, the considerable progress in experimental instrumentation and nuclear theory suggest that a re-examination now could be very fruitful, especially regarding the largely unstudied structure at higher angular momentum. In particular, most previous experiments used light ion beams and provided very little information on the highest-spin states possible below the neutron separation energies. There was also only limited information on intruder states and their structures.

^{25}Na is accessible through proton pickup from ^{26}Mg and di-neutron transfer to ^{23}Na. Almost all previous investigations of the excited states in ^{25}Na have used these two approaches. Both the ^{26}Mg(d,^{3}He) [1–3] and the ^{26}Mg(t,α) [4–7] reactions provided proton pickup results, while the ^{23}Na(t,p) [4, 5, 8] reaction was used to study di-neutron pickup. Angular distributions were measured for the outgoing light particle in many of these studies and were analyzed with transfer models, such as the distorted-wave Born approximation (DWBA) to determine spins and spectroscopic factors. Polarized deuterons were used in one case [3] to unambiguously determine J. Gamma decays were also observed [5–7], providing more accurate level energies, spin assignments through angular distribution measurements, and lifetimes from the Doppler-shift attenuation method (DSAM). Completely different decay modes were reported [5, 7] for the 3995 keV state, as will be discussed below. Finally an investigation of the ^{25}Mg β decay to states in ^{25}Na provided further information [9] on a few states.

Many states had been reported up to relatively high energies, but no information existed on the electromagnetic decays of states above 4300 keV in ^{25}Na although the neutron separation energy S_n of 9.011 MeV would allow γ decay from much higher-lying states. Furthermore, no states of spin greater than 9/2 $\hbar$ had been observed. In the present work, the more symmetric ^{9}Be(^{18}O,pnγ)^{25}Na reaction was used to investigate the existence and decay properties of higher-spin states.

^{21}F is also accessible through proton pickup from ^{22}Ne, although only one such experiment ^{22}Ne(t,α) [10] has been reported, likely due to the inconvience of the target. Much more popular has been the ^{19}F(t,p) di-neutron transfer [4, 11–14]. Rather unusual was the

^{22}Ne(α,^{2}He) di-neutron transfer reaction [15]. The ^{7}Li(^{18}O,$\alpha\gamma$) reaction was used to measure the lifetime of the lowest $9/2^{+}$ level. [16]. A measurement of the γ decays following β decay of the $5/2^{+}$ ground state (g.s.) of ^{21}O has also provided valuable information on the structure of ^{21}F [17]. No γ decays had been reported for states above 4600 keV prior to the present work, even though the neutron threshold lies at 8.1 MeV. The ^{9}Be(^{14}C,pnγ) reaction was used in the present work to investigate higher spin states in ^{21}F

II. EXPERIMENTAL PROCEDURE

Beams of ^{18}O and long-lived radioactive ^{14}C from the FSU tandem accelerator were incident on an 0.5 mm thick ^{9}Be target in two separate experiments to populate ^{21}F and ^{25}Na. This target was thick enough to stop the primary beam, but allowed decay protons and α particles to pass through with limited energy loss. Protons were detected and identified in an E-ΔE Si detector telescope placed co-linear with the beam 5 mm downstream of the Be target. Gamma decays were detected in coincidence with the protons in the FSU array. Two Compton-suppressed single-crystal Ge detectors of about 25% efficiency were placed at 35°, two at 90°, and three at 145°. Three 4-crystal Compton-suppressed "clover" detectors were also placed at 90°. In the analysis the detected energies of hits in more than one crystal of a clover were added together because such multiple hits were dominated by Compton scattering betweem the crystals.

An ^{18}O beam energy of 35 MeV was used for the ^{9}Be(^{18}O,pnγ)^{25}Na reaction. Three Si detectors, each 1480 μm thick and 1.5 cm in diameter were centered at 0° relative to the beam. The first was used as a ΔE detector and the sum of the other two was used as the E signal for particle identification. Signals were processed using convential fast-slow analog electronics. The Compton supression and particle-γ coincidence logic was performed in a custom-built trigger circuit.

^{14}C beam energies of 30, 35, and 45 MeV were used for different parts of the ^{9}Be(^{14}C,pnγ) experiment. Charged particles were detected and identified with a 1000 μm thick Si E detector and a 100 μm thick ΔE one. A thinner 0.125 mm Be target was used for part of this experiment to reduce the α attenuation, although this had little effect on the protons. All of this data was used in the analysis after proper adjustment of parameters for the different energies and target thicknesses. In this later experiment, a newly acquired Compton-supressed

80% efficient Ge detector replaced one of the smaller detectors at 145°. Also the analog data acquisition system was replaced with a digital XIA PIXE16 system with custom firmware for the Compton supression and particle-γ coincidence logic [18].

In the subsequent off-line analysis for both experiments, gammas in coincidence with protons selected by their dE/dx values in the telescope were sorted into 1-D spectra (primarily to study g.s. decays) and 2-D matrices. Doppler correction presented more of a challenge because of the slowing down of the recoils in the thick targets as they were decaying. To work with this, three matrices were formed for each experiment with 0, 1, or both axes approximately corrected for the average Doppler shifting of the faster transitions and the other axes left uncorrected. Also matrices with detectors at only one angle on one axis were formed for analysis of angular distributions and for lineshapes for the Doppler-shift attenuation lifetime analyses.

Since $\cos^2(35°) = \cos^2(145°)$, our array gives only two independent values for γ angular distributions (35°/145° and 90°). This has the advantage of yielding better statistical accuracy at the two points, but allows a determination of only the a_2 coefficient in the Legendre expansion

$$Y(\theta) = A_0(1 + a_2 P_2(cos\theta)),$$

assuming that the P_4 term is small. a_2 values should be -0.32 (+0.45) for a pure M1 (E2) decay with the alignment in these reactions of $\sigma = 0.5\hbar$. However, the limitation in all angular distribution measurements is that M1 transitions can have a significant admixture of E2 decay, measured by δ. The value of a_2 for a mixed M1/E2 transition can vary between +0.5 and -1.0 for δ values between -0.5 and +0.5 [19].

Lifetimes were determined for a number of the decay lines in the two nuclei by comparing the Doppler-shifted lineshapes (Doppler-shift attenuation method DSAM) in the thick Be targets with simulations of the slowing down and decay process. Stopping powers for the slowing down of both the incident beam and the recoiling nuclei were calculated by SRIM [20]. A feeding model was used which assumes a feeding time which decreases linearly with excitation energy starting at zero at the neutron separation. The slopes were fitted to a few previously determined lifetimes for each nucleus. The feeding times used were

$$T(E_x) = A * E_x(keV) + B$$

where E_x refers to the excitation energy of the state, and A = -3.48 E-5 ps/keV (-4.46 E-5

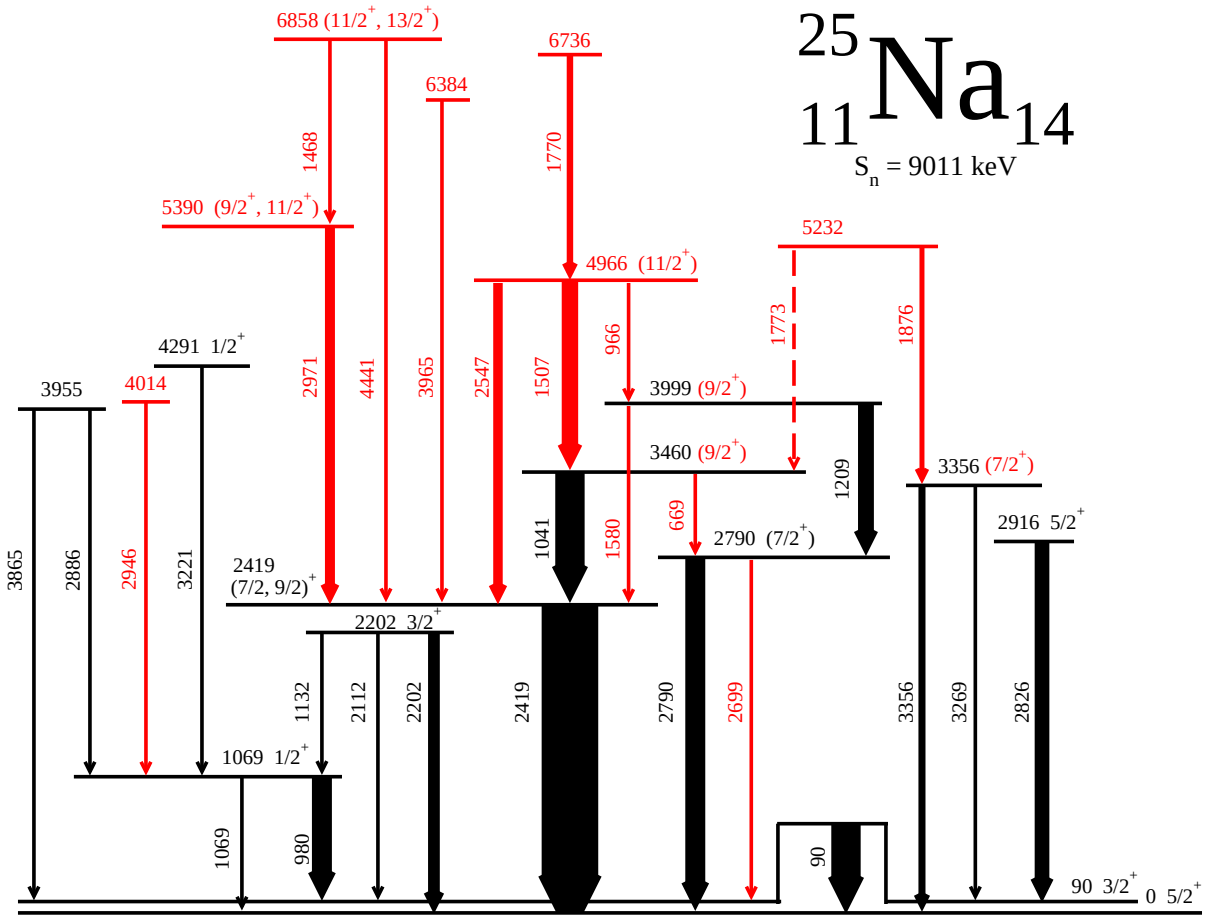

FIG. 1. (Color online) The level and decay scheme of ^{25}Na based on the present data. States and transitions in red are new to this work; transition widths are proportional to the observed intensities.

ps/keV) and B = 0.32 ps (0.37 ps) for ^{25}Na (^{21}F).

III. RESULTS

A. ^{25}Na

Results from the present experiment are displayed in the level scheme of Figure 1 and in Table I. States and transitions not previously reported are shown in red in all figures. The present work is in agreement with previous results for states below 2400 keV. Some comments are appropriate for states above this.

The most intense decay line observed in the present experiment is the ground state (g.s.)

TABLE I. Excitation energies, transition energies, intensities, angular distribution coefficients, and mean lifetimes in ^{25}Na.

E_x (keV)	E_γ (keV)	$2J_i$ ($\hbar$)	$2J_f$ ($\hbar$)	I_γ	a_2	τ present (fs)	τ previous (fs)
89.7(3)	89.7(3)	3^+	5^+	50(10)	-0.56(9)		7400(400)[a]
1069.3(3)	1069.3(3)	1^+	5^+	3.4(3)		1750(200)	1800(200)[b]
	979.7(2)		3^+	34(2)			
2202.4(2)	2202.3(3)	3^+	5^+	20(2)	-0.08(9)	25(15)	36(6) [b]
	2112.2(4)		3^+	4.7(5)			
	1132.4(3)		1^+	13(1)	-0.30(9)	25(15)	36(6) [b]
2419(1)	2419(1)	$(9)^+$	5^+	100	0.27(9)	240(40)	200(140)[a]
2790(1)	2790(1)	$(7)^+$	5^+	34(2)	0.02(9)	190(35)	250(50) [b]
	2699(1)		3^+	3.0(3)			
2916(1)	2826(1)	5^+	3^+	25(2)	0.39(9)	60(40)	15(5)[b]
3356(1)	3356(1)	$(7)^+$	5^+	12(1)	0.01(9)		
	3269(3)		3^+	1.6(2)			
3460(1)	1041(1)	$(9)^+$	$(9)^+$	50(3)	0.28(9)	130(40)	210(25)[b]
	668.6(5)		$(7)^+$	3.6(2)	-0.67(8)		
3955(1)	3865(1)		3^+	3.9(3)			
	2886(2)		1^+	2.3(2)			
3999(1)	1580(1)	$(9)^+$	$(9)^+$	3.7(3)			
	1209(1)		$(7)^+$	27(1)	-0.38(9)	100(20)	
4014(2)	2946(2)		1^+	1.4(1)			
4291(1)	3221(1)	1^+	1^+	1.9(2)			
4966(2)	2547(1)	$(11)^+$	$(9)^+$	10.9(6)	0.14(9)	120(30)	
	1507(1)		$(9)^+$	28(2)	-0.60(8)	80(20)	
	966(1)		$(9)^+$	3.3(3)			
5232(3)	1876(1)		$(9)^+$	8.4(5)			
	1773(3)		$(9)^+$	(2.4(7))			

TABLE I. *Continued.*

E_x (keV)	E_γ (keV)	$2J_i$ ($\hbar$)	$2J_f$ ($\hbar$)	I_γ	a_2	τ present (fs)	τ previous (fs)
5390(2)	2971(1)	$(9,11)^+$	$(7,9)^+$	17(1)	-0.15(9)		
6384(4)	3965(3)		$(7,9)^+$	4.5(5)			
6736(3)	1770(1)		$(11)^+$	11(1)	0.21(9)		
6858(3)	4441(2)	$(11,13)^+$	$(7,9)^+$	3.9(4)			
	1468(1)		$(9,11)^+$	3.8(3)	-0.87(14)		

[a] Ref. [6]
[b] Ref. [7]

decay from the 2419 keV state. The proton pickup ℓ value of 4 $\hbar$ in the ^{26}Mg(d,^{3}He) reaction to the 2419 keV state provided a J^π assignment of $7/2^+$ or $9/2^+$ [1]. The facts that the 2419 keV state is the most strongly populated in the ^{9}Be(^{18}O,pn) reaction which favors higher spin states and that neither the present nor any previous experiment has observed any other decay branch than to the $5/2^+$ g.s. tend to favor the higher $9/2^+$ assignment which would preclude decay to the 90 keV $3/2^+$ level. Six transitions (only one previously known) have been observed decaying into the 2419 keV state, as shown in Figure 2.

In contrast to the 2419 keV level, a decay has been newly observed from the 2790 keV state to the 90 keV $3/2^+$ level. This limits the maximum spin of the 2790 keV state to $7/2^+$, consistent with the $J^\pi = 3/2^+$ or $7/2^+$ asssignment in the ^{23}Na(t,pγ) reaction [6]. The presently measured a_2 anisotropy coefficient for the stronger g.s. transition implies M1 decay, supporting the $3/2^+$ or $7/2^+$ assignment. Newly observed transitions of 669 and 1580 keV show that the 3460 and 3999 keV states decay to both the 2419 and 2790 keV levels, strongly suggesting the higher spin possibility of $7/2^+$ for the latter level.

The angular distribution of the g.s. decay of the 3356 keV state implies a $\Delta J = 1$ transition and J^π of $3/2^+$ or $7/2^+$. The $7/2^+$ possibility is more likely given the newly observed feeding into this state connected with the higher spin structure. The only observed decays from the 3460 keV state are the previously known 1041 keV transition to the 2419 keV level and the newly observed 669 keV one to the 2790 keV level. The 1041 keV angular distribution is consistent with either a $\Delta J = 0$ or 1 transition, while the large negative a_2

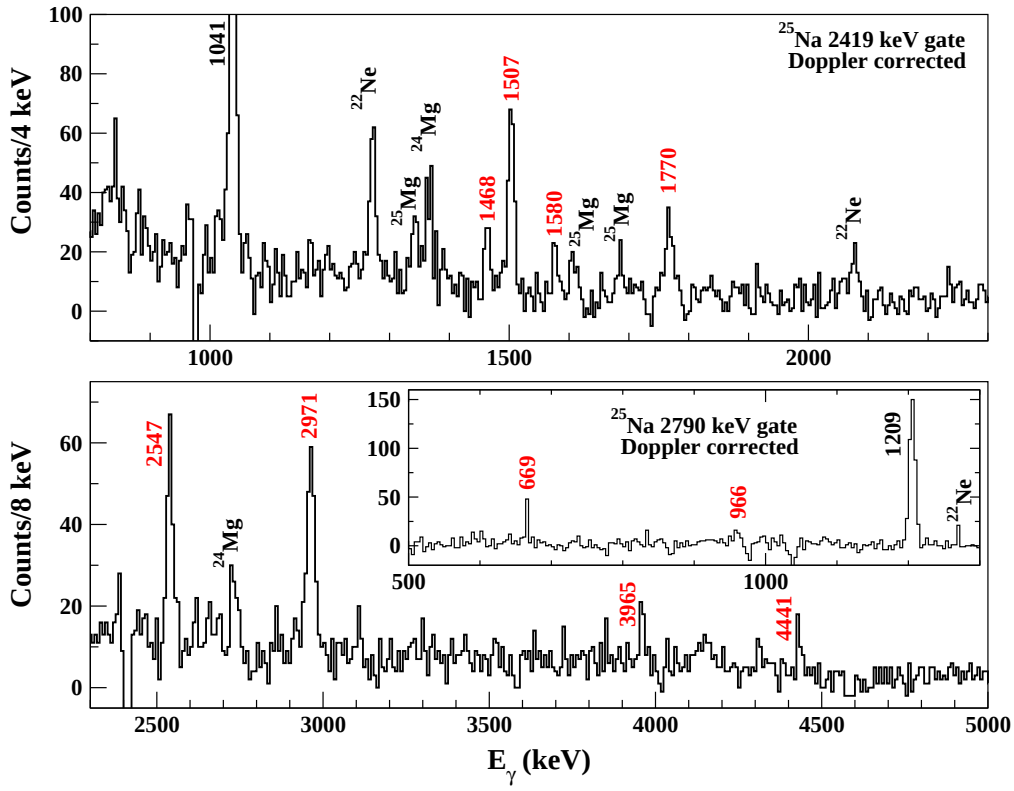

FIG. 2. (Color online) Portions of the γ spectra in coincidence with the 2419 and 2790 (inset) keV lines. Red labels are used for newly observed γ peaks.

coefficient for the 669 keV one is only consistent with $\Delta J = 1$. Due to the relatively strong population of the 3460 keV state in the present reaction which favors higher spin states and the lack of any decay branches to any lower spin levels below 2419 keV, $J^\pi = 9/2^+$ is very likely for this state.

Two different γ decay modes have been reported for a state or states near 4 MeV. One mode is a single decay branch to the 2790 keV state observed in the ^{23}Na(t,p) di-neutron pickup reaction [5]. The other mode is 3 different decays to the $1/2^+$ level at 1069 keV and to the $3/2^+$ levels at 90 and 2202 keV observed in the ^{26}Mg(t,α) proton pickup reaction [7]. A spin-parity of $1/2^-$ was assigned to a state at 3995 keV based on a clear $\ell = 1\ \hbar$ angular distribution in the ^{26}Mg(d,^{3}He) proton pickup reaction [2, 3]. Decays to the $1/2^+$ and $3/2^+$ levels are exactly what would be expected from the lowest $1/2^-$ state.

In the present work, no evidence has been seen for decays from a state near 4 MeV to any of the $1/2^+$ or $3/2^+$ levels (See Fig. 3). Rather, we see the 1209 keV decay line to the 2790 keV state (See inset in Fig. 2), as previously reported [7], and a new 1580 keV decay

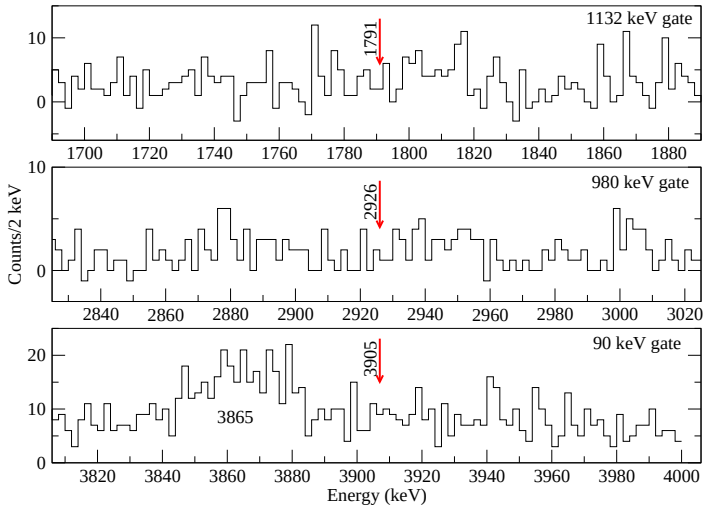

FIG. 3. (Color online) Portions of gated γ spectra around the energies of previously reported decays of the 3995 $1/2^-$ state in ^{25}Na.

to the 2419 keV level. This situation is best explained by a doublet of states very near 4 MeV. One has spin $1/2^-$, excitation energy about 3995 keV, and decays to all the states below it consistent with E1 decay. The other, populated in different reactions including the present ^{9}Be(^{18}O,pn) one, has positive parity, relatively high spin, and decays only to the highest spin states below it. The a_2 coefficient measured in the present work for the 1209 keV line implies a relatively unmixed M1 transition and $J^\pi = 9/2^+$ for the 3999 keV state.

A new state at 4966 keV was established by 3 newly observed decays to the 3 very likely $9/2^+$ levels below it. The a_2 value for the 1507 keV decay restricts it to M1. This would assign $11/2^+$ to the 4966 keV state and is consistent with the a_2 value for the 2547 keV decay, which implies $\Delta J = 0$ or 1.

A newly observed 1876 keV decay line to the 3356 keV level establishes a state at 5232 keV. Although no angular distribution information could be inferred for this weaker line, its decay to the very likely $7/2^+$ level limits its spin to $7/2^+$ - $11/2^+$. There is likely another decay branch to the 3460 keV level. However, the energy of this line, 1773 keV, is too close to the 1770 keV line from the 6736 keV state to resolve it and there is no possible coincidence gate to separate the 1773 keV line. The 1773 keV decay is implied only by intensity measurements from the combined 1770-1773 keV gate which show greater intensity for the 1041 and 2419 keV lines than for the 1507 one.

A 5390 keV state is established by newly observed decays into and out of it. The a_2 value

of its decay to the 2419 keV level implies an M1 transition and $11/2^+$ ($9/2^+$) for the very likely (rather unlikely) assignment of $9/2^+$ ($7/2^+$) for the 2419 keV state.

New states are assigned at 6384 and 6736 keV by newly observed decays to the 2419 and 4966 keV levels, respectively. Angular distribution information could not restrict the spin assignments, but their decays place spin limits of $9/2^+$ to $13/2^+$ and $11/2^+$ to $15/2^+$, respectively.

The highest state observed in the present work, at 6858 keV, is established by two newly observed decays. The a_2 value of the 1468 keV line is only consistent with M1 decay, implying $13/2^+$ or, less likely, $11/2^+$.

Some sample DSAM lineshape fits are shown in Figure 4 and the lifetimes which could be measured are listed in Table I.

B. ^{21}F

The experimental results from the ^{9}Be(^{14}C,pnγ) reaction are summarized in the level scheme of Figure 5 and in Table II.

The present experiment provides new results for states above 2 MeV. As shown in Figure 6, a number of newly observed γ decays end on the 1755 keV state, which has the highest previously assigned spin, suggesting the preferential population of higher spin states. A weak 2(1)% new decay branch was observed from the 2036 keV $3/2^-$ state to the 1102 keV $1/2^-$ level. It is a litte surprising that the M1 decay branch is so weak compared to the E1 decays. A new 3(2)% decay branch was observed from the 2068 keV state to the 1102 keV $1/2^-$ level, suggesting a parallel with the 2036 keV $3/2^-$ state. A spin-parity of $5/2^-$ was suggested for the 2068 keV state [17], and further model dependent justification for this assignment will be discussed below. A number of newly discovered transitions decay into the 2068 keV state, as can be seen in Figure 7. Before the present work, no decays had been observed from these $3/2^-$ and ($5/2^-$) states to the only negative parity state below them, the 1102 keV $1/2^-$ one. This lack of selectivity for decay to $\pi = -$ states also appears to apply to two higher $\pi = -$ states to be discussed below.

A new 12(1)% g.s. decay branch was observed from the 3635 keV state in addition to the previously known decay to the lowest $9/2^+$ level. The a_2 value of the latter decay is consistent with $9/2^+$ or $7/2^+$ for the parent level. We confirm decays from the 4566 keV state

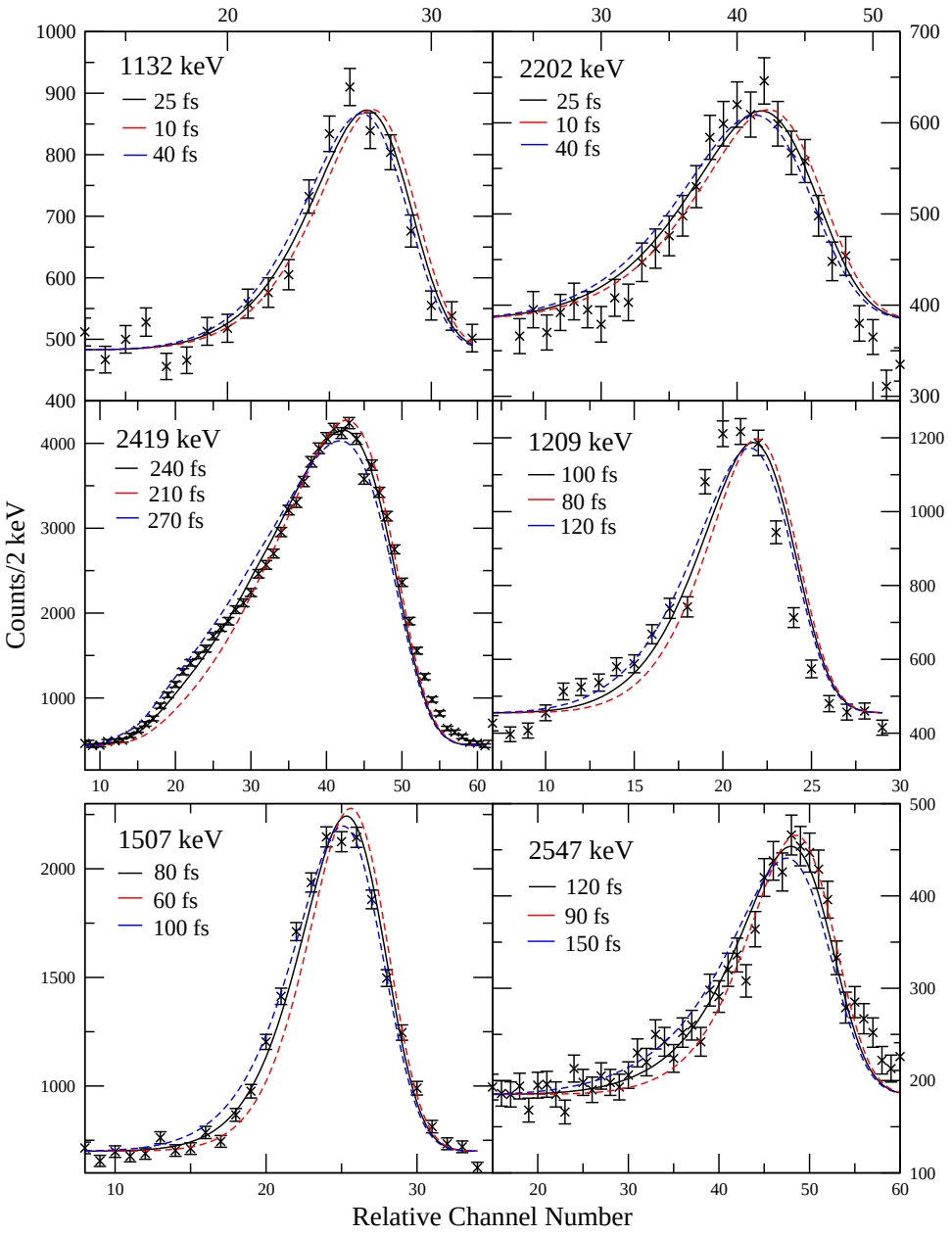

FIG. 4. (Color online) Some sample DSAM lineshapes and fits for transitions in ^{25}Na. The black curves represent the best overall fits, while the red and blue curves indicate the one standard deviation uncertainties.

to the 3635 and 1755 keV levels. The evidence is consistent with the previous suggestion of $7/2^+$ [17]. The newly observed 4664 and 4895 keV states decay only to relatively high spin states and are produced more strongly in the present reaction which favors higher spin states than other states seen more strongly in earlier work. These strongly suggest higher

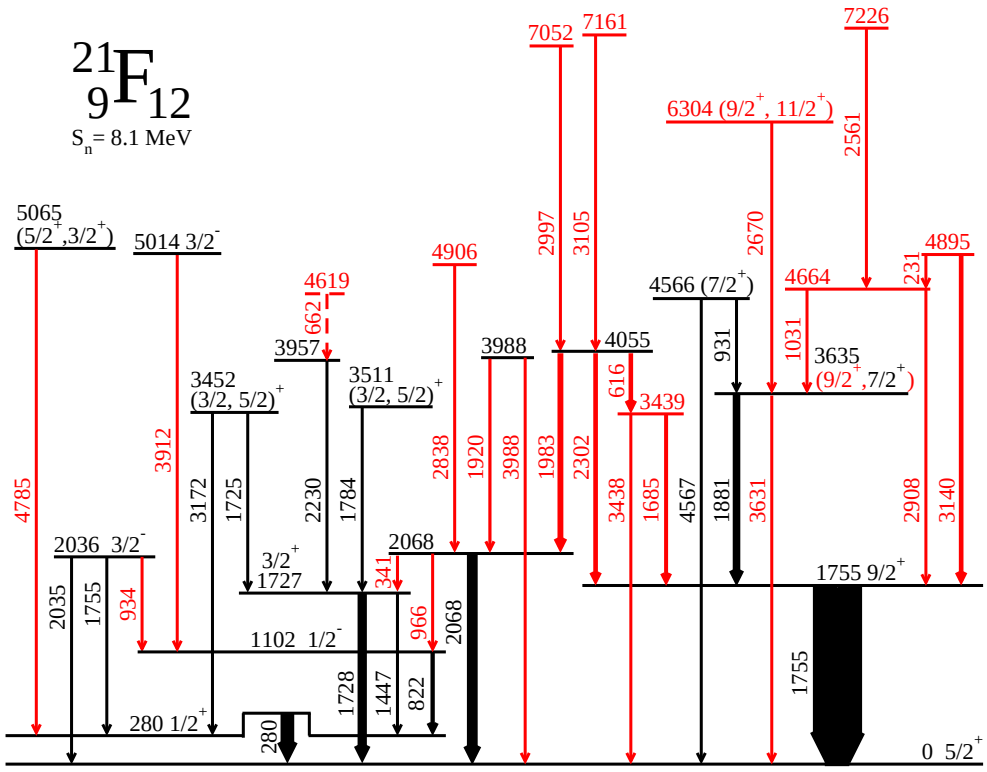

FIG. 5. (Color online) The level and decay scheme of ^{21}F based on the present data. States and transitions in red are new to this work; transition widths are proportional to the observed intensities.

spin, likely greater than $9/2^+$ but no higher than $13/2^+$. The a_2 value of the connecting 231 keV line implies an M1 transition. Two more newly observed states at 6304 and 7226 keV also decay to the higher spin group of states rising from the 1755 $9/2^+$ state. They very likely have positive parity and spins of $9/2^+$ or greater.

A group of five states at 3988, 4055, 4906, 7052, and 7161 keV, many newly observed, have decay paths which end on the 2068 keV state, tentatively assigned $5/2^-$. Particularly interesting are the 3988 - 4055 keV and 7052 - 7161 keV doublets, which resemble the 2036 - 2068 keV one. Model interpretations of these states will be discussed below.

Some representative DSAM fits for decay lineshapes in ^{21}F are shown in Fig. 8.

IV. DISCUSSION

There are both similarities and differences between the two $T_z = 3/2$ nuclei studied here, ^{21}F and ^{25}Na. Past studies have used primarily di-neutron transfer to the stable isotope or

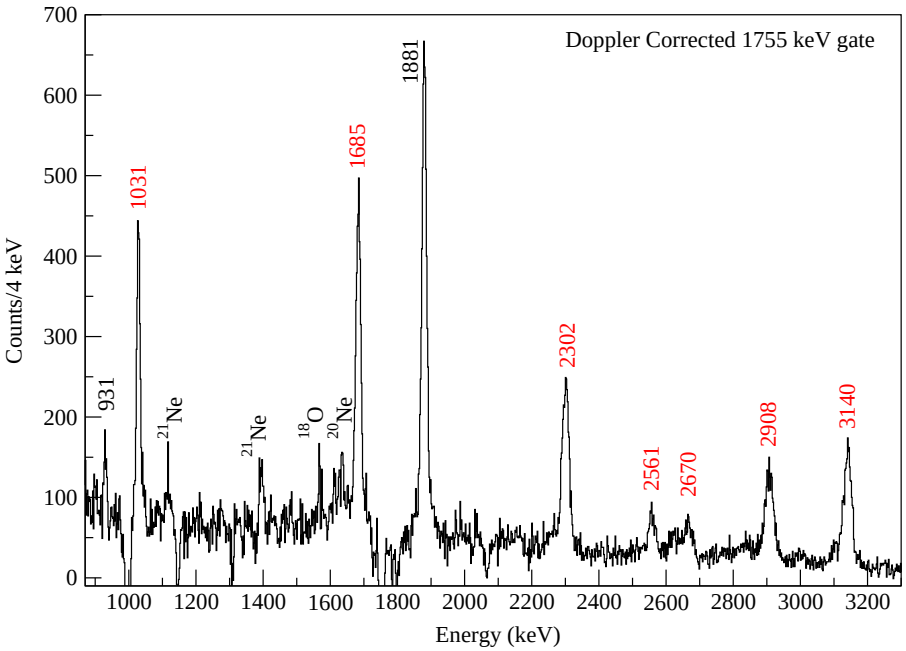

FIG. 6. (Color online) A portion of the γ spectrum in coincidence with the 1755 keV line in ^{21}F.

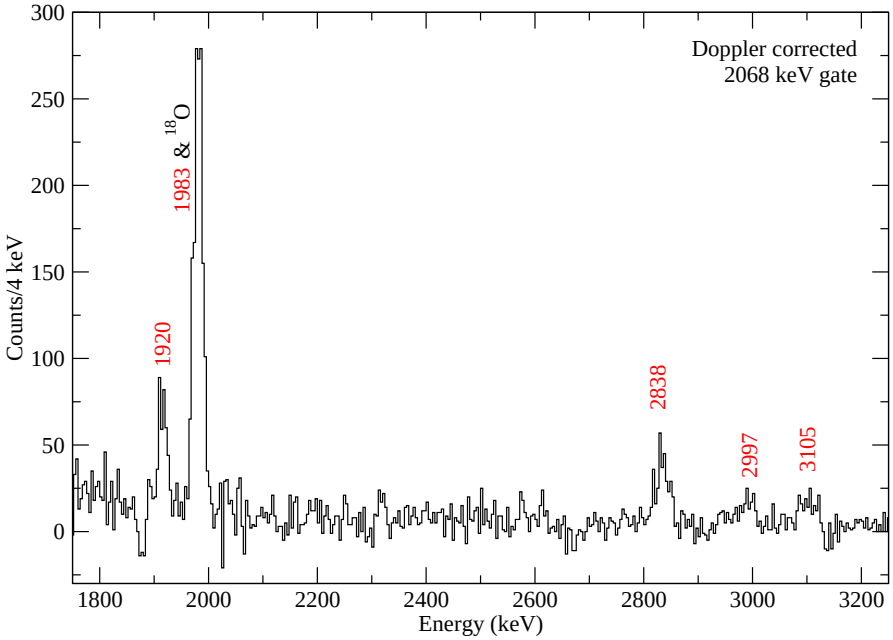

FIG. 7. (Color online) A portion of the γ spectrum in coincidence with the 2068 keV line in ^{21}F. Analysis of the uncompressed spectrum shows that about 1/3 of the 1983 keV peak comes from ^{21}F.

TABLE II. Excitation energies, transition energies, intensities, angular distribution coefficients, and mean lifetimes in ^{21}F.

Ex (keV)	E_γ (keV)	I_γ	a_2	τ present (fs)	τ previous (fs)
280.0(6)	280.0(6)	27(1)	0		8.31(26) [a]
1102.3(7)	822.4(4)	8.7(9)	-0.02(9)	440(45)	440(8) [b]
1727.1(8)	1727.5(6)	19(2)	0.34(9)	60(35)	70(60) [b]
	1446.7(5)	4.1(3)		40(35)	
1754.7(8)	1754.7(8)	100	0.61(9)		3500(500) [c]
2036(1)	2035(2)	5.5(10)	0.35(9)		<500 [b]
	1755(1)	3.2(3)			
	934(1)	0.2(1)			
2068(1)	2068(1)	22(1)		100(30)	80(30) [b]
	966(2)	0.7(5)			
	340.8(3)	0.9(2)			
3439(1)	3438(2)	4.6(3)			
	1685(1)	8.2(4)			
3452(2)	3172(1)	1.1(1)		<150	<1000 [b]
	1725(2)	0.8(1)			
3511(1)	1784(1)	1.7(2)			
3635(2)	3631(4)	2.0(1)		175(40)	
	1881(1)	15.6(5)	0.06(9)		
3957(2)	2230(1)	0.3(1)			
3988(3)	3988(3)	6.3(3)			
	1920(2)	6.4(8)			
4055(2)	2302(1)	10.8(10)	0.55(9)	160(35)	
	1983(2)	12(2)			
	615.8(5)	9.3(5)			

TABLE II. Excitation energies, transition energies, intensities, angular distribution coefficients, and mean lifetimes in ^{21}F (continued).

Ex (keV)	E_γ (keV)	I_γ	a_2	τ present (fs)	τ previous (fs)
4566(3)	4566(2)	1.2(3)			
	931(1)	1.5(2)			
4619(3)	662(1)	4.4(8)			
4664(3)	2908(2)	6.1(3)		70(30)	
	1031(1)	5.2(2)			
4895(3)	3140(2)	9.5(5)	-0.94(9)	260(80)	
	231.4(5)	1.9(3)			
4906(4)	2838(3)	4.3(6)			
5014(4)	3912(3)	0.7(1)			
5065(3)	4785(3)	1.3(2)			
6304(4)	2670(3)	2.4(3)	-0.52(9)		
7052(5)	2997(3)	1.0(3)			
7161(6)	3105(5)	1.2(2)			
7226(4)	2561(2)	2.4(2)			

[a] in ns Ref. [13]
[b] Ref. [14]
[c] Ref. [7]

single proton pickup from another stable nucleus and have tended to populate the lower spin states. By contrast, the experiments used here involved the fusion of more symmetric beam-target combinations, followed by mostly statistical evaporation and favoring the population of higher spin states. Also use of a more modern gamma detector array combined with coincident proton detection has allowed exploration of the electromagnetic decay properties of higher lying states in these lesser known, more neutron-rich nuclei. One difference between the two nuclei is the position of the lowest negative-parity state. The $1/2^-$ state lies at only 1102 keV in ^{21}F (low $\pi = -$ states are common in the F isotopes), compared to nearly 4

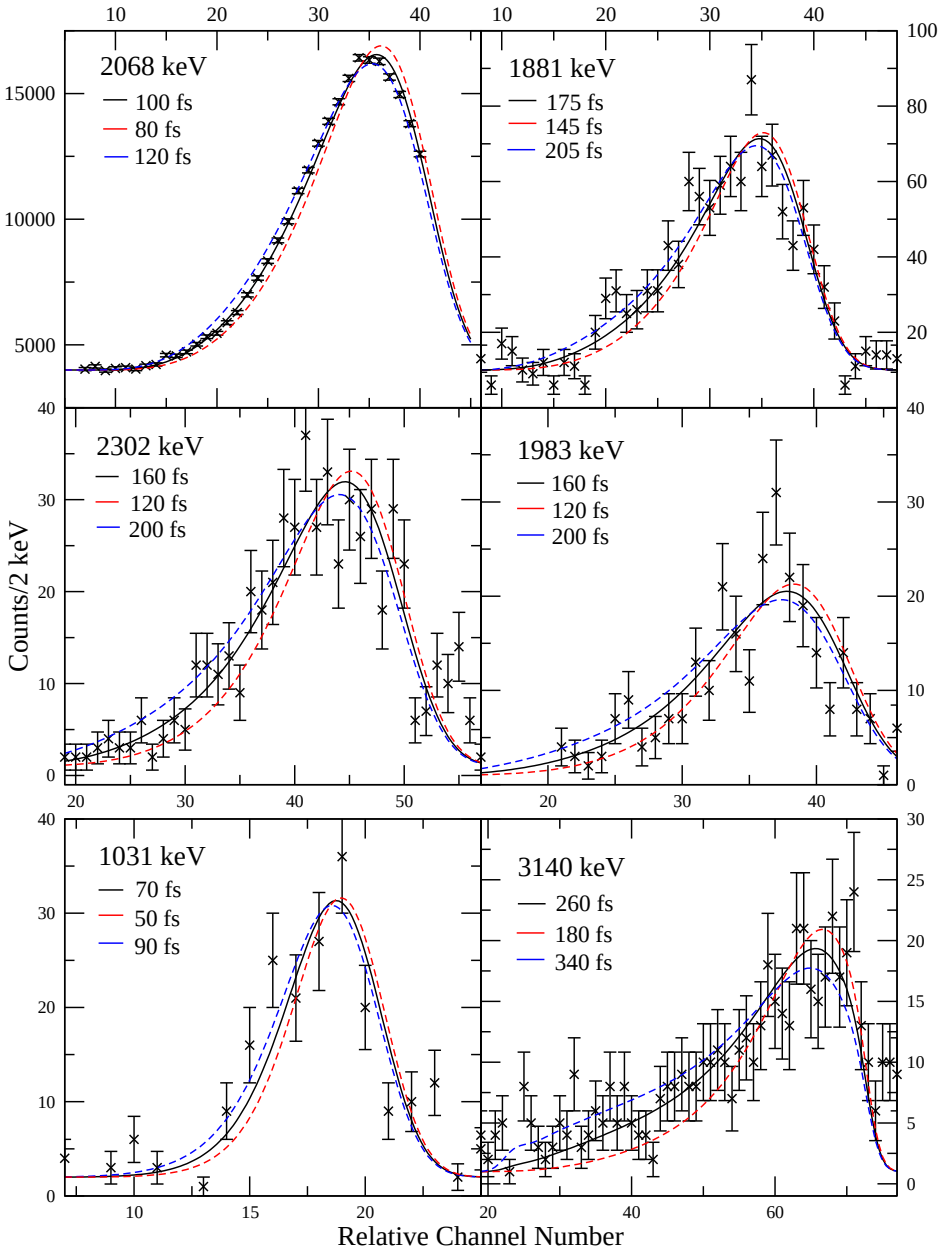

FIG. 8. (Color online) Some sample DSAM lineshapes and fits for transitions in ^{21}F. The black curves represent the best overall fits, while the red and blue curves indicate the one standard deviation uncertainties.

times the excitation energy (3995 keV) in ^{25}Na [2, 3]. The result is that we saw no sign of population of negative-parity states in ^{25}Na in contrast to almost equal population of the states of both parities in ^{21}F. And the two nuclei differ in composition by only one α particle!

We have presented above what can be determined about spin-parity assignments from

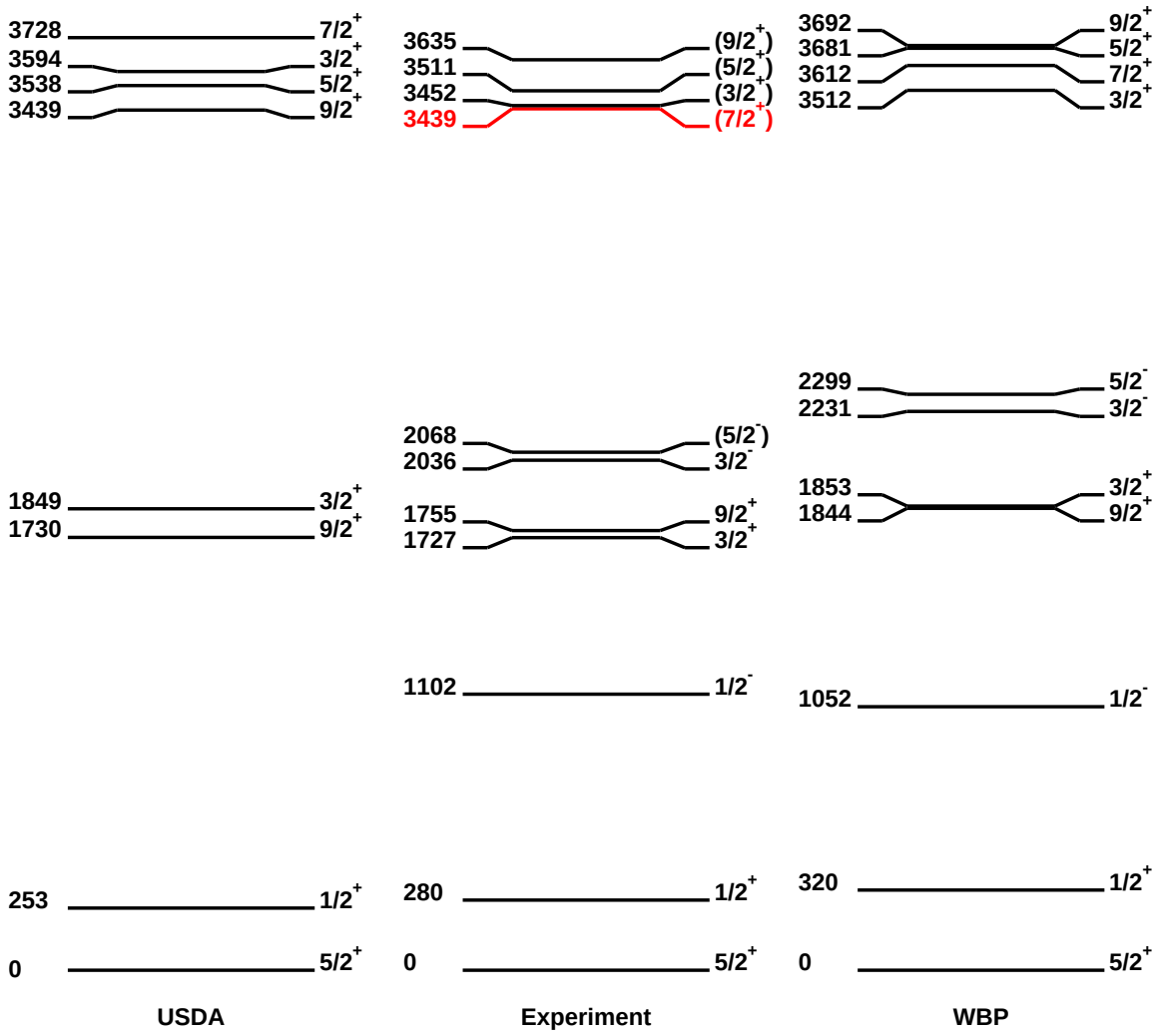

FIG. 9. (Color online) Comparison of lower experimental energy levels in ^{21}F with two shell model calculations using the indicated interactions. Partially model-dependent spin assignments are shown in parentheses and newly reported energy levels are colored red.

both the present and previous work. In the following comparison with relevant theory calculations, we will present more model-dependent spin-parity proposals which we believe are very likely. These are shown in blue color in the figures.

As will be discussed below, all the positive-parity states appear to be well represented by shell model calculations using the "universal" s-d (USD) interaction [21] which is used for 0p-0h states in the WBP interaction or a more recent adjustment of this effective interaction called USDA [22] calculated in the pure s-d model space. That is, all particles above N=Z=8 are allowed to occupy the $0d_{5/2}$, $1s_{1/2}$, and $0d_{3/2}$ orbitals and couple in all possible ways. All such states have positive parity. Negative parity states must involve an odd number

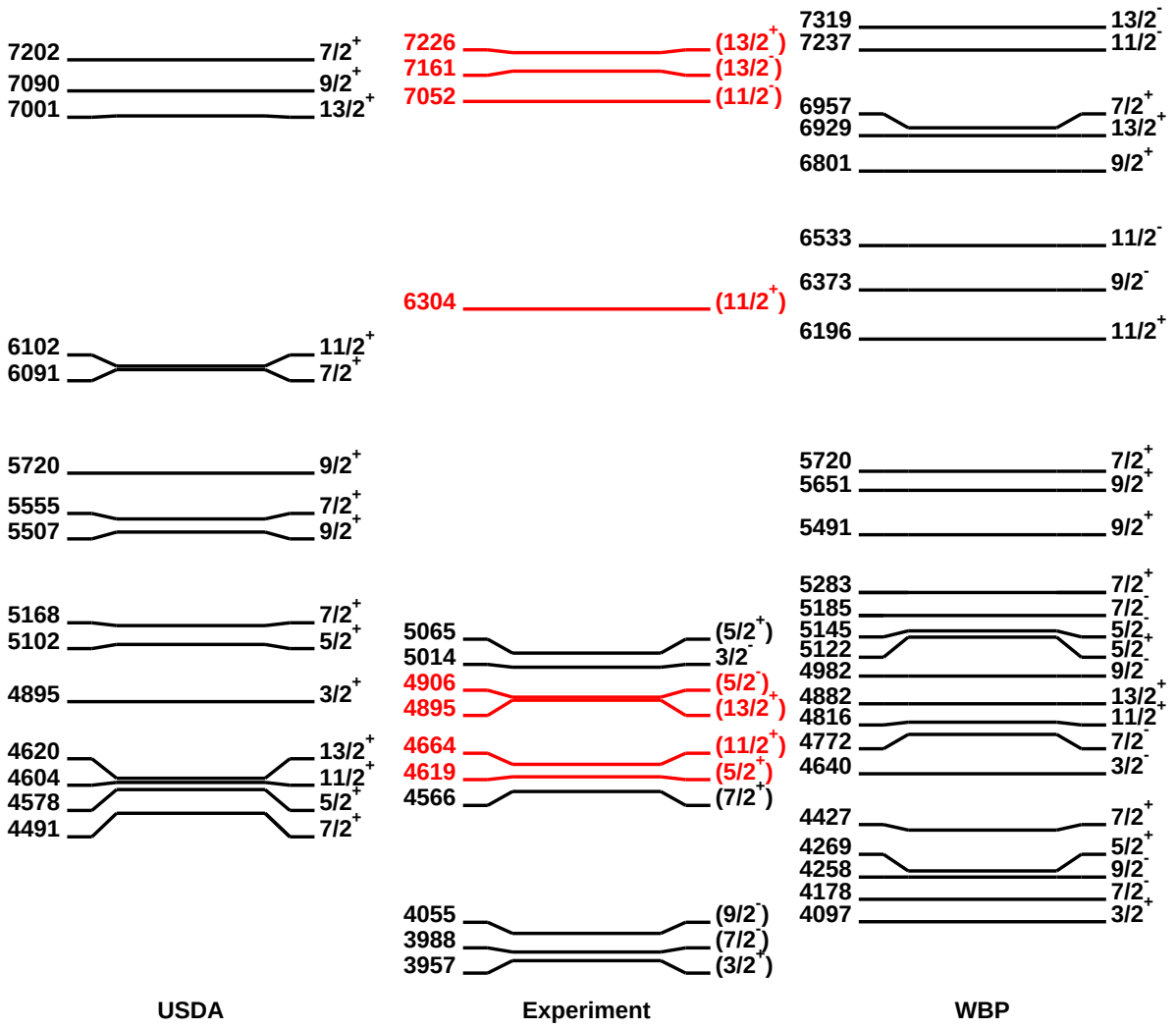

FIG. 10. (Color online) Comparison of higher experimental energy levels in ^{21}F with two shell model calculations using the indicated interactions. Partially model-dependent spin assignments are shown in parentheses and newly reported energy levels are colored red.

of particles promoted from the 0p shell below or into the 0f-1p shell above. The WBP interaction [23] has been used for these calculations with only 1 intruder particle allowed in either the 0p or 1p-0f orbitals. For both nuclei, it was found that the negative-parity states arise predominately from intruders due to the promotion of nucleons out of the $0p_{1/2}$ orbital rather than excitations out of the s-d shell.

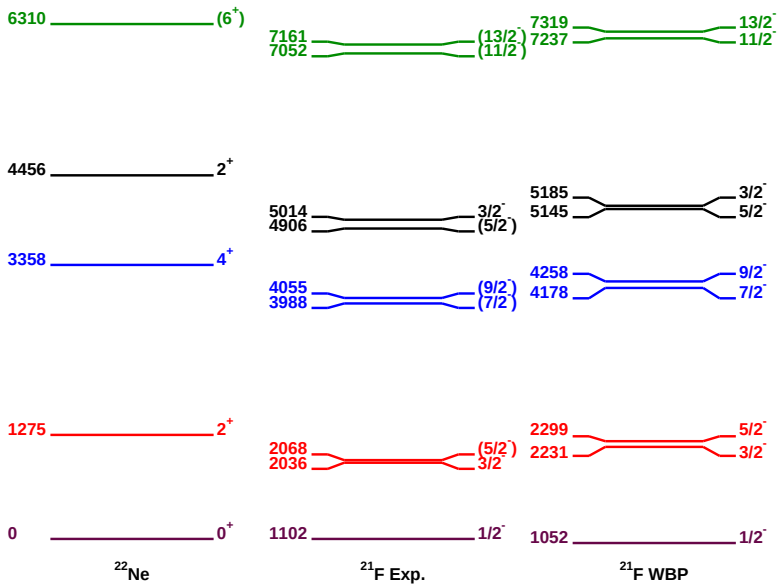

FIG. 11. (Color online) Comparison of lowest excited states in ^{22}Ne with negative-parity states in ^{21}F and 1p-1h shell model calculations using the WBP interaction. The levels in ^{22}Ne are color-coded to match the corresponding states in experiment and the WBP shell-model calculations.

A. ^{21}F

The experimental results are compared with two shell model calculations in Figs. 9 and 10. In these figures the most likely experimental candidates have been matched with theoretical states. While these matches cannot give absolutely certain spin assignments, they are consistent with all the experimental spin restrictions, and there is a good theoretical candidate for each π=+ state with both interactions and for each π=- state in the 1-particle-1-hole (1p-1h) WBP calculations. The root-mean-square (RMS) differences between experiment and theory are about 160 keV for both the WBP and USDA interactions among the positive-parity states. This is about as accurate as shell model calculations get for such a range of states and the agreement extends up to the highest spins possible in this excitation energy range, $13/2^+$ and $13/2^-$. The RMS differences for the negative-parity states compared to WBP calculations are only slightly higher at about 190 keV . The B(E2) transition strengths agree rather well with both the WBP and USDA calculations, as shown in Table III. Standard effective charges of 1.5 e (0.5 e) were used for protons (neutrons) for the B(E2) calculations. The B(M1) strengths predicted by the two interactions are very similar, but tend to overpredict the experimental values in most cases. The E(1) strengths

TABLE III. Experimental and theoretical electromagnetic transition strengths B(Tλ) in ^{21}F. The experimental B(M1) values have been computed assuming zero mixing ratio δ. Note that transitions involving negative-parity states can only be calculated with the WBP interaction, since the USDA interaction does not allow cross-shell excitations.

Ex	E_γ	Tλ	exp.	USDA	WBP
keV	keV		W.u.	W.u.	W.u.
280	280	E2	16.6(3)	17.2	17.5
1102	822	E1	5.24(11) E-3		0.123
1727	1728	M1	$0.27^{+0.38}_{-0.10}$	1.21	1.30
	1447	M1	$0.10^{+0.13}_{-0.04}$	0.32	0.29
1755	1755	E2	$4.1^{+0.6}_{-0.3}$	4.71	4.65
2068	2068	E1	$1.3^{+0.6}_{-0.3}$ E-3		0.084
	966	E2	84^{+36}_{-20}		15.6
	341	E1	$1.6^{+0.7}_{-0.3}$ E-2		0.045
3452	3172	M1	0.01(1)	0.24	0.23
	1725	M1	$0.05^{+0.01}_{-0.03}$	1.24	1.26
3635	3631	E2	0.24(5)	0.20	0.19
	1881	M1	$0.024^{+0.007}_{-0.004}$	0.021	0.026
4055	2302	E1	$2.2^{+0.8}_{-0.4}$ E-4		0.046
	1983	E2	$17.3^{+4.6}_{-2.9}$		18.0
	616	E1	$1.2^{+0.4}_{-0.2}$ E-2		0.043
4664	2908	M1	$0.03^{+0.02}_{-0.01}$	0.053	0.058
	1031	M1	$0.6^{+0.4}_{-0.2}$	1.0	1.1
4895	3140	E2	$2.3^{+0.9}_{-0.6}$	3.0	3.0
	231	M1	$5.4^{+2.4}_{-1.3}$	0.46	0.54

from the cross shell calculations with the WBP interaction are significantly overpredicted.

An alternative model assuming weak coupling appears equally successful in describing the negative-parity states in ^{21}F. In this picture, the negative parity states resemble a $0p_{1/2}$ hole coupled to low-lying states of ^{22}Ne. It implies degenerate doublets of J-1/2 and J+1/2

when coupled to ^{22}Ne states of spin J (except for J = 0, where only $J^\pi = 1/2^-$ is possible). The result is shown graphically in Fig. 11 which compares ^{22}Ne states with the negative-parity levels in ^{21}F and those predicted with the WBP interaction. The close spacing of the negative-parity J$\pm$1/2 doublets in ^{21}F and the similarity of their energies to the lowest states in ^{22}Ne strongly supports the weak coupling interpretation. The correspondence with the WBP results indicates that the shell model calculations contain essentially the same physics.

B. ^{25}Na

The experimental level scheme of ^{25}Na observed in the present experiment was compared with shell model calculations using the USDA and WBP interactions in Fig. 12. The spins indicated in blue for the experimental states are consistent with all the experimental decay information, but not uniquely determined. These model-dependent assignments give the best agreement between experiment and theory up to $13/2^+$ states. The RMS differences with the USDA results are quite comparable to those in ^{21}F at 140 keV, while those with the WBP interaction (based on the older USD interaction for 0p-0h states) are somewhat higher at 260 keV. Experimental electromagnetic transition strengths and those calculated with the shell model using the USDA and WBP interactions with E2 effective charges of 1.5 e (0.5 e) for protons (neutrons) are shown in Table IV. There is reasonably good agreement with experiment for both the M1 and E2 strengths.

No previously reported negative-parity states were observed in the present experiment, and good matches exist among the positive-parity states predicted by the shell model for all the observed states. As discussed earlier, we concluded the existence of a doublet of states near 4 MeV, one a moderately high-spin positive-parity level observed in the present work and the other, a $1/2^-$ one not populated in this experiment. The fact that the lowest negative-parity state in ^{25}Na lies at almost four times the energy of the one in ^{21}F means the ^{25}Na negative-parity states are far from yrast, leading to very much lower population in the present predominantly fusion-evaporation reaction. A few negative parity states have been reported before. These are compared with 1p-1h calculations using the WBP interaction and with states in ^{26}Mg for signs of weak coupling to a $0p_{1/2}$ hole in Fig. 13. The WBP results do resemble the weak coupling picture, but not enough experimental states are known to

TABLE IV. Experimental and theoretical electromagnetic transition strengths B(Tλ) in ^{25}Na. The experimental B(M1) values have been computed assuming zero mixing ratio δ.

Ex	E_γ	Tλ	exp.	USDA	WBP
keV	keV		W.u.	W.u.	W.u.
90	90	M1	0.020(2)	0.025	.040
1069	1069	E2	6.8(7)	10.25	7.92
	980	M1	0.06(1)	0.001	0.015
2202	2202	M1	$0.20^{+0.77)}_{-0.10}$	0.19	0.22
	2112(4)	M1	$0.05^{+0.20}_{-0.03}$	0.063	0.026
	1132(3)	M1	$0.99^{+3.72}_{-0.49}$	0.12	0.12
2419	2419	E2	$9.4^{+1.8}_{-1.4}$	10.4	10.2
2790	2790	M1	0.02(1)	0.0035	0.0063
	2699	E2	0.5(2)	1.01	0.15
2916	2826	M1	$0.08^{+0.18}_{-0.03}$	0.33	0.30
3460	1041	M1	$0.65^{+0.25}_{-0.14}$	0.079	0.010
	669	M1	$0.18^{+0.07}_{-0.04}$	0.050	0.042
3999	1580	M1	$0.03^{+0.02}_{-0.01}$	0.035	0.036
	1209	M1	$0.51^{+0.29}_{-0.13}$	0.061	0.051
4966	2547	M1	0.01(1)	0.026	0.020
	1507	M1	$0.18^{+0.19}_{-0.6}$	0.035	0.037
	966	M1	$0.08^{+0.09}_{-0.03}$	0.0018	0.0058

draw any conclusions, due in part to favoring of low-spin states in previous reactions.

V. SUMMARY

Substantial new experimental information has been measured on the nuclear structure of $T_Z = 3/2$ ^{21}F and ^{25}Na formed in heavy-ion fusion-evaporation reactions and detected in an array of Compton suppressed Ge spectrometers with proton detection for exit channel selection. These experiments have favored the states of higher spin, complementary to most earlier investigations. The current experiments observed many new states and electromag-

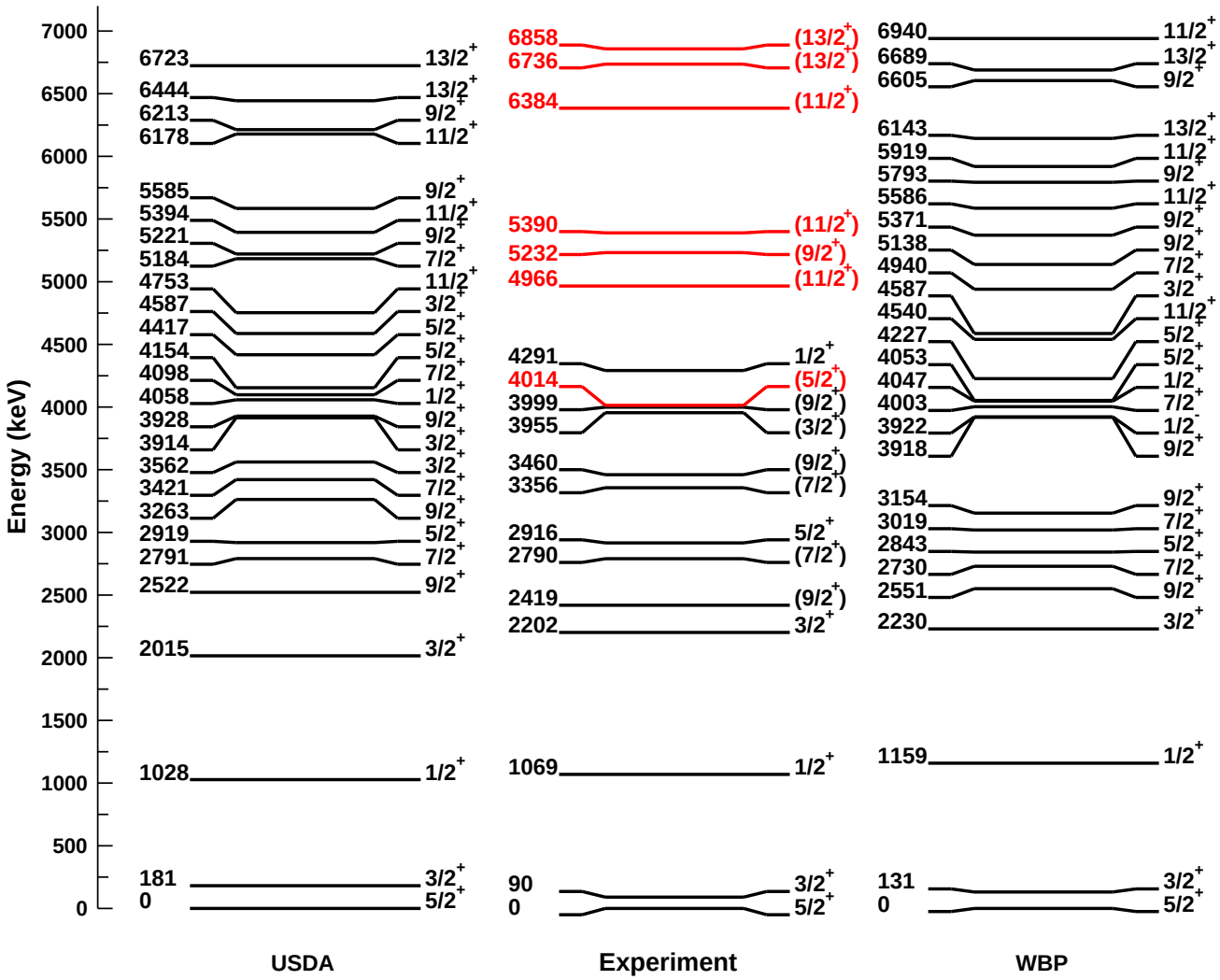

FIG. 12. (Color online) Comparison of experimental energies levels in ^{25}Na with two shell model calculations using the indicated interactions. Partially model-dependent spin assignments are shown in parentheses and newly reported energy levels are colored red.

netic decays, along with their angular distributions and DSAM lifetimes where possible. States of probable spin 13/2 $\hbar$ were seen around 7 MeV excitation in both nuclei.

The energies of the positive-parity levels in both nuclei are rather well reproduced by shell model calculations restricted to the s-d shell. Agreement is best for the USDA interaction, a newer fit to many more energy levels in the s-d shell. In fact the RMS deviations of 140-160 keV for both nuclei are about as good as are seen anywhere in the shell. This agreement extends from the lowest to the highest spins. There is generally good agreement with the

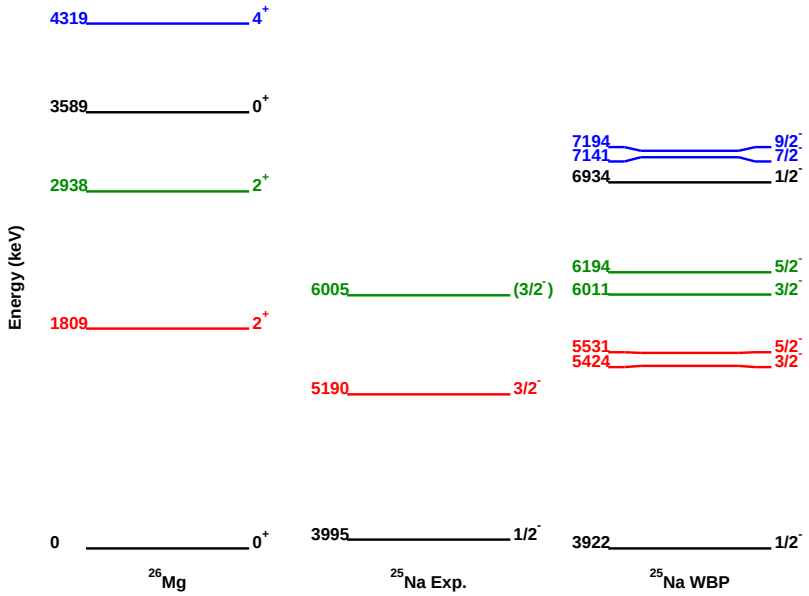

FIG. 13. (Color online) Comparison of lowest excited states in ^{26}Mg with negative-parity states in ^{25}Na reported in the literature and 1p-1h shell model calculations using the WBP interaction. The levels in ^{26}Mg are color-coded to match the corresponding states in experiment and the WBP shell-model calculations.

E2 transition strengths, while agreement with the M1 strengths is reasonable, but not quite as good. The E1 strengths in ^{21}F are overpredicted by the WBP interaction. No evidence is seen for significant influence of fp configurations in the negative-parity levels, as occurs for the more neutron-rich isotopes.

Two differences were observed with the negative-parity states in ^{21}F. One is that they start at much lower excitation energies (1102 keV) than in other s-d shell nuclei. In fact, lower than would be expected for the typical p-sd shell gap. The other is their tendency to decay at least as strongly to positive-parity states, when decay to negative-parity states is energetically comparable. Even so, any decay branch to a π = - level appears to be an indicator of negative parity. Theoretically, the excitation energies of these π = - states are relatively well reproduced by 1p-1h calculations using the WBP interaction. Also the weak coupling approximation assuming a $0p_{1/2}$ hole coupled to the low lying states in ^{22}Ne works well, as shown by the closely spaced doublets built on all non-zero spin ^{22}Ne states (30 - 100 keV spacing) and the agreement with both experiment and the WBP calculations. In contrast, the lowest negative-parity state in ^{25}Na has been shown to lie at about 4 MeV, but neither this nor any other negative-parity state was observed in the present experiment.

ACKNOWLEDGMENTS

This work was supported in part by U.S. National Science Foundation grants 1064819 and 1401574. We are grateful to Sean Liddick for providing us with his software for reading the XIA system.

---

[1] J. Jänecke, Nucl. Phys. **A204**, 497 (1973).

[2] E. Krämer, G. Mairle, and G. Kaschl, Nucl. Phys. **A165**, 353 (1971).

[3] T. Kihm, *et al.*, Zeit. Phys. **318**, 205 (1984).

[4] S. Hinds, R. Marchant, and R. Middleton,Nucl. Phys. **31**, 118 (1962).

[5] J.A. Becker, R.E. McDonald, L.F. Chase, Jr., and D. Kohler, Phys. Rev. **188**, 1783 (1969).

[6] R. Bertini, *et al.*, Nucl. Phys. **A283**, 64 (1977).

[7] R.L. Kozub, *et al.*, Nucl. Phys. **A403**, 155 (1983).

[8] H.T. Fortune, R. Middleton, J.D. Garrett, and R.M. Dreizler, Phys. Lett. **79B**, 56 (1978).

[9] David R. Goosman, D. E. Alburger, and J.C. Hardy, Phys. Rev. C **7**, 1133 (1973).

[10] M. G. Silbert and Nelson Jarmie, Phys. Rev. **123**, 221 (1961).

[11] Nelson Jarmie, Phys. Rev. **104**, 1683 (1956).

[12] P. Horvat, Nucl. Phys. **52**, 410 (1964).

[13] R.E. McDonald and J. A. Becker, Phys. Rev. **154**, 1101 (1967).

[14] E.K. Warburton and J.W. Olness, Phys. Rev. C **2**, 2235 (1970).

[15] P. von Neumann-Cosel *et al.*, Phys. Rev. C **56**, 547 (1997).

[16] R.L. Kozub *et al.*, Phys. Rev. C **27**, 158 (1983).

[17] D.E. Alburger *et al.*, Phys. Rev. C **23**, 2217 (1981).

[18] http://www.xia.com (2015).

[19] J.M. VonMoss, Ph.D. Dissertation, Florida State University (2015).

[20] http://www.srim.org (2008); J. F. Ziegler, J. P. Biersack, and U. Littmark, *The Stopping and Range of Ions in Matter*, (Pergamon, New York, 1985).

[21] B.A. Brown and B.H. Wildenthal, Annu. Rev. Nucl. Part. Sci. **38**, 29 (1988).

[22] B.A. Brown and W.A. Richter, Phys. Rev. C **74**, 034315 (2006).

[23] E.K. Warburton and B.A. Brown, Phys. Rev. C **46**, 923 (1992).